Sensitivity Analysis of the Effect of Pore Structure and Geometry on Petrophysical and Electrical Properties of Tight Media: Random Network Modeling

Faisal Alreshedan[1*] and Apostolos Kantzas[1, 2]

[1] Department of Chemical and Petroleum Engineering, University of Calgary, Calgary, Canada
[2] PERM Inc. TIPM Laboratory, Calgary, Canada

ABSTRACT

Several methodologies published in the literature can be used to construct realistic pore networks for simple rocks, whereas in complex pore geometry formations, as formed in tight reservoirs, such a construction still remains a challenge. A basic understanding of pore structure and topology is essential to overcome the challenges associated with the pore scale modeling of tight porous media. A stochastic random generation algorithm was employed to assess the effects of certain pore structure and geometries on the estimation of petrophysical and electrical properties of tight media through physically realistic 3D random networks. A Weibull truncated equation was used to predict the distribution of network pores and throats. An equivalent 3D pore network of Berea Sandstone was generated based on published pore and throat size distributions. The estimated porosity, absolute permeability, and formation factor of the reconstructed pore network are in good agreement with published laboratory measurements. Moreover, the estimated drainage and imbibition relative permeability curves are in a good match with corresponding experimental relative permeability curves. Subsequently, the effect of pore structure on basic core properties is evaluated by varying the Berea network pore size, throat size, and coordination number (connectivity) distributions. Finally, the effect of pore and throat geometries on two phase flow properties is investigated. The study shows the importance of taking into consideration the internal pore structure for petrophysical and electrical properties estimation.

Keywords: Tight Media, 3D Random Network, Weibull Truncated Equation, Berea Sandstone, Pore Structure and Geometries

INTRODUCTION

The main objective of experimental analyses is to reduce uncertainty in reservoir evaluation by obtaining representative reservoir microscopic and macroscopic properties under reservoir conditions. However, laboratory measurements, especially in tight porous media, are costly and time consuming. Also, studying the effect of a certain parameter in such complex pore structures is difficult, due to the complexity associated with the experimental setup. As an alternative approach, pore network modeling can be used to construct physically sound models of a real porous media. Pore network modeling gives a reasonable prediction of fluid

*** Corresponding author**
Faisal Alreshedan
Email: fsreshed@ucalgary.ca
Tel: +14 03 9184252
Fax: +14 03 2825060

Article history
Received: December 09, 2014
Received in revised form: April 04, 2015
Accepted: May 11, 2015
Available online: January 23, 2016

flow properties at the pore scale, and offers the flexibility of studying the macroscopic properties relationship with pore structure and geometries.

In pore network modeling, the complex pore structure in a rock is represented by a network of pore-bodies (void spaces) and pore-throats (narrow paths that connect pore-bodies) with simplified geometries. When this is successfully established, then single and multi-phase flow calculations can be performed [1, 2]. Detailed physics and productive capabilities for pore-scale modeling of multiphase flow on the pore scale have been reviewed in several studies [3-5]. At the early stages of network modeling, Fatt predicted capillary pressure and relative permeability curves of drainage using two-dimensional (2D) regular lattice networks, where the radii was randomly assigned [6]. He found that the network lattice yielded closer agreement to experimental measurements than assuming the porous media as a bundle of parallel tubes. Later, Chatzis and Dullien [7] reviewed Fatt's network model work and they illustrated that 3D pore network models represent the real porous media more realistically than 2D pore network models. Following this early work, extensive studies on the importance of topology, pore bodies and throats size distribution, and their spatial correlations were performed [7-11]. However, most of these studies were based on regular lattice networks, which are limited in reflecting the real topology and geometry of a rock. The capabilities of network modeling were enormously improved and have been applied to making many successful predictions of single and multi-phase flow and transport properties, including two and three-phase relative permeability and capillary pressure of conventional formations [12-18]. In complex sandstones, it is recommended that a 3D-image-based representation of the pore space, which should capture the statistics of the real rock, should first be created. This can be generated using a direct imaging technique such as micro-CT scanning [1, 2] or by various process/object-based modeling approaches [12-14, 19]. Subsequently, using various image based network extraction techniques [20, 21], an equivalent pore network is then extracted from the 3D image to estimate the single and multiphase fluid flow properties. Several authors have found that it is not practical to calculate the multiphase fluid flow properties directly, using for example Lattice-Boltzmann, through physically 3D images, because it is very computationally expensive [22-24].

The pore topology/structure of unconventional reservoirs, particularly tight gas, is unlike conventional reservoirs. In the literature, a tight gas reservoir is characterized by a dual porosity model, in which secondary pores represent the large fraction of void spaces connected to each other by slots. These slots have an important effect on permeability, as well as on gas flow through tight porous media; but, they may not have a significant contribution to porosity [25-27]. In order to replicate the pore topology/structure of tight gas reservoirs and model fluid flow through such porous media, one needs to know the constitutive relationships between the macroscopic properties of the system.

The main objective of this paper is to use a random network modeling approach for a better understanding of the effect of selected pore structure (pore radius and throat radius and connectivity) and geometries (circular, square, and triangular cross-section) on macroscopic properties in permeable and tight porous media. A Weibull truncated equation is used to determine the distribution of network element properties such as pore/throat radius, length, shape factor, and coordination number (number of pore throats per pore body). The connectivity between pores is established in a similar procedure as given by Idowu [28]. A 3D pore network of Berea sandstone is constructed and the estimated macroscopic properties are validated with published experimental measurements. The purpose of this exercise is to confirm that the networks used in

this work are not radically different than those presented previously in the literature. Then, the effect of pore structure and geometries on estimating porosity, absolute permeability, and formation factor are inferred by constructing a number of different networks. Furthermore, the predicted formation factor-permeability, formation factor-porosity, and permeability-porosity relationships are discussed. A detailed data analysis is presented in the following sections.

Pore Network Modeling

Imperial College's stochastic random network generation software developed by Idowu [28] is used as a starting point in this research. The software requires the knowledge of network element properties of pores and throats (radius, length, volume, shape factor, and connectivity), which can be obtained using image based network extraction techniques. The primary advantage of his approach is that it can be used to generate an arbitrarily-sized network. However, extracting geometrically equivalent network properties based on representative high resolution images for complex pore structures is computationally very expensive [28-31]. Consequently, a Weibull truncated equation is used herein to estimate the distribution of network elements properties (pore/throat radius, length, shape factor, and coordination number). This distribution was proved to be the most adequate one for network modeling applications of sandstones as early as the 1980's, because it can establish a non-zero frequency for the minimum and maximum values of pore and throat sizes [32, 33]. The Weibull truncated equation is given by:

$$x = (x_{max} - x_{min}) \times \left\{-\delta ln\left[R\left(1-e^{-1/\delta}\right)+e^{-1/\delta}\right]\right\} + x_{min} \quad (1)$$

where, x is the estimated property value and x_{min} and x_{max} are the minimum and maximum values of x property respectively; δ and γ are Weibull exponents, which define the shape of Weibull distribution. Furthermore, the area, volume, and clay volume of each network element are calculated using the following equations [18, 34]:

$$A = \frac{r^2}{4G} \quad (2)$$

$$V = AL \quad (3)$$

$$Clayvol = \frac{V.Clayper}{(1 - Clayper)} \quad (4)$$

where, A is the area, r is the radius, and G is the dimensionless shape factor and its value depends on selected pore and throat geometries; L is the length of pore or throat, *Clayvol* is the estimated clay volume for each element, and *Clayper* is the clay proportion, which is an input to the program. It should be noted that consistent units e.g. micrometers or meters should be used. The connectivity between pores is established in a similar procedure as the one described by Idowu [28]. The maximum length condition and correlation function between two connected pores are utilized.

In this study, an Imperial College program called Pore-Scale Modeling [18, 34] is used to estimate the petrophysical and electrical properties of the constructed pore networks. The program is a quasi-static simulator of two-phase capillary dominated flow following the work of Ören et al. [14] and Patzek [15]. The software simulates primary drainage, wettability alteration, and any subsequent cycles of imbibition and secondary drainage. No trapping mechanism is implemented during primary drainage, whereas a snap-off trapping mechanism is considered during imbibition. The program assumes water saturated clays will not be drained during fluid displacements, and it is rather considered as a constant clay volume associated with each element, which remains water-filled.

Berea Sandstone

The network construction procedure is validated by generating an equivalent network of Berea sandstone with dimensions of (3x3x3) mm^3

consisting of 12,349 pores. The estimated petrophysical properties are in good agreement with the published experimental data of Berea sandstone [35] as shown in Table 1. The input parameters used are selected according to the extracted network properties presented by Idowu [28]. The input minimum and maximum values for each element property (radius, length, and shape factor) are read directly from the extracted distribution, where the Weibull exponent parameters for pore and throat radius are estimated using a back calculation procedure assuming the values of δ and γ until the best visual match between the estimated and extracted distribution is achieved as shown in Figures 1 and 2 respectively. However, the distribution of extracted pore and throat lengths and coordination number do not follow the Weibull distribution function. Thus the exponent parameters are assumed and altered manually for a better match in petrophysical and electrical properties with the laboratory measurements. That justifies the variation between the estimated values with the reported values by Al-Dhahli et al. [35] as shown in Table 1. Typical values of δ and γ used in this work vary between 0.001 to 1 for δ and between 0.1 to 5 for γ.

Table 1: Estimated network parameters of Berea sand.

Parameters	Al-Dhahli et al. [35]	This work
Permeability (md)	2673	2518
Net Porosity (%)	18.3	18.4
Clay Porosity (%)	5.72	6.0
Formation Factor	15.16	12.4

The measured porosity was 18% and clay proportion was 9% [13].

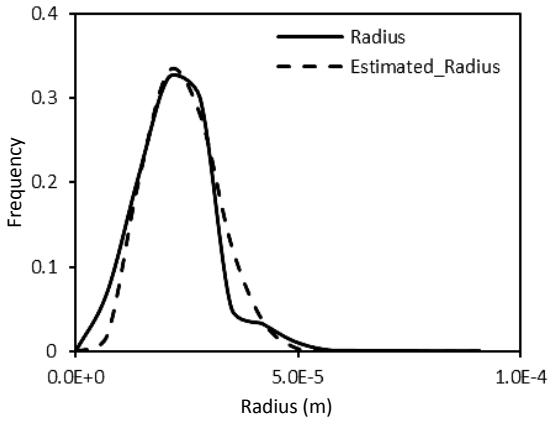

Figure 1: Weibull estimation of pore size distribution is in good agreement with the original extracted distribution.

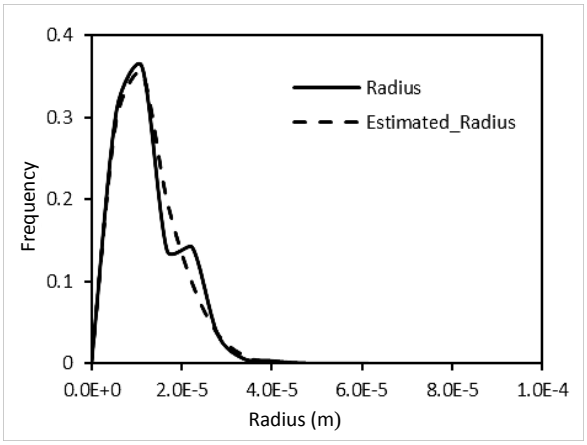

Figure 2: Weibull estimation of throat size distribution is in good agreement with the original extracted distribution.

The number of connected throats/branches for each pore (i.e. coordination number) and the length of pore and throat have an impact on the estimation of petrophysical and electrical properties. On the other hand, a good match was achieved between the estimated and experimental relative permeability curves for both drainage and imbibition displacements as shown in Figures 3 and 4 respectively. The estimated resistivity index and capillary pressure curves during drainage and imbibition displacements are shown in Figures 5 and 6 respectively. The corresponding lab measurements of those curves are not available to be validated. Table 2 lists the input fluid parameters used for modeling two-phase flow (water/oil) through a porous

medium. The values presented by Al Dhali et al. [35] are included for reference purposes.

The sensitivity analysis is conducted based on the equivalent network of Berea sandstone to study the effect of pore throat structure and geometries on porosity, absolute permeability, and formation factor estimation. A detail data analysis and finding is presented in the following sections.

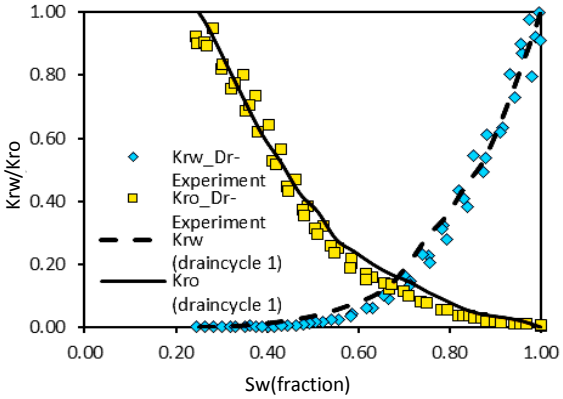

Figure 3: Comparison of the measured and estimated two phase relative permeability curves in Berea sandstone for drainage.

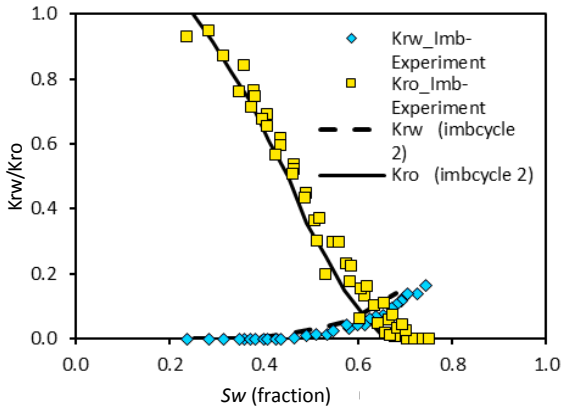

Figure 4: Comparison of the measured and estimated two phase relative permeability curves in Berea sandstone for imbibitions.

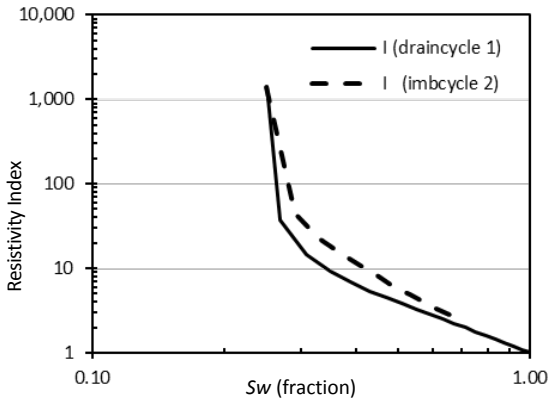

Figure 5: Estimated resistivity index in Berea sandstone for drainage and imbibition.

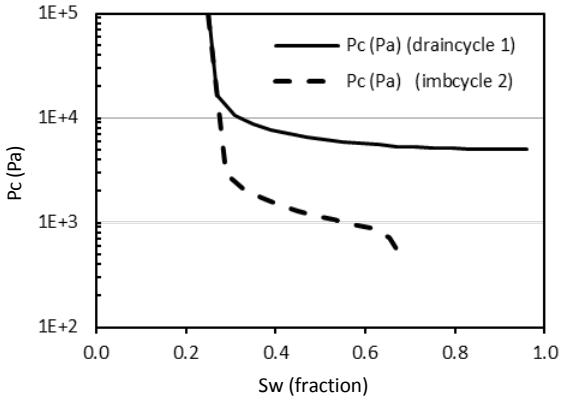

Figure 6: Estimated capillary pressure in Berea sandstone for drainage and imbibition.

Pore Structure Effects

The objective is herein achieved by shifting each element of the pore structure (pore size, throat size, and coordination number) independently, combining two elements, and combining all three elements together in order to produce realistic tight porous media. The input parameters used to construct a 3D network of Berea sandstone is served as a reference to the generated networks in this study. In the reference network, a zero clay fraction is assumed. The impact of this assumption is that all wetting phase is potentially displaceable.

Table 2: Input fluid parameters used for modeling two-phase flow (water/oil) through a porous medium.

	Contact Angle, Drainage	Contact Angle, Imbibition	IFT (m.N/m)	Oil Viscosity (m.Pas)	Water Viscosity (m.Pas)
This Work	0	50-60	48	1.36	1.05
Al Dhahli et al. [35]	0	20-72	48	1.39	1.05

Also, if clay type pore sizes are to be considered, they have to be part of the pore size distribution, when a displacement is modeled. It is further assumed that the pore length is $2r_p$ (pore radius) instead of using a Weibull distribution. This assumption is made to limit this sensitivity analysis on these three factors. Seven networks are generated by varying only the values of Weibull exponent parameters (δ and γ) for pore and throat radius and coordination number without manipulating their minimum and maximum values. Figure 7 shows the reduced distributions with the original distributions of the reference network. Table 3 illustrates the variation in net porosity, absolute permeability, formation factor obtained by running Pore-Scale Modeling software and using Archie's equation to estimate the cementation exponent (m) by assuming a=1.0.

$$F = a\emptyset^{-m} \quad (5)$$

where, F is formation factor, Φ is porosity, m is the cementation exponent, and α is the Archie's constant (including tortuosity, it is herein assumed to be one).

From Table 3 it can be seen that the reference network gives a lower estimate for porosity, absolute permeability, and formation factor than the 3D network of Berea sandstone (Table 1). This reduction is due to the assumption employed for calculating pore length ($L_p = 2r_p$) of the reference network. Consequently, the distribution of pore length in reference network is lower than in Berea sandstone network. The choice of sensitivity analysis parameters aims at adjusting network properties towards formations much tighter than Berea sandstone. The data in Table 3 are not meant to provide specific experimental matching, but are to demonstrate trends on core properties with changing pore parameters.

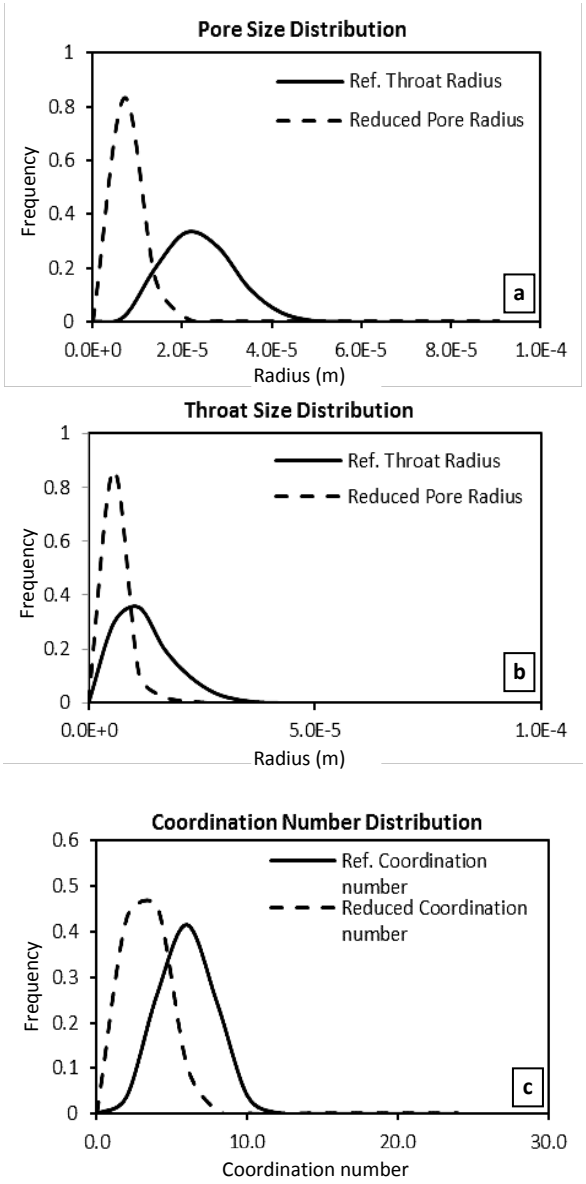

Figure 7: The reduced distributions of tested factors plotted with the reference distributions used for generating a 3D network of Berea sandstone.

Figure 8 (a) shows the net porosity values for all the cases plotted in Cartesian coordinates. It can clearly been seen that when the distribution of pore radius is reduced independently, the estimated porosity dropped from 15.3% to 1.0%. Permeability by definition measures the connectivity of a porous media and all three pore structure factors contribute to the fluid flow. Thus the estimated absolute permeability declined in all the cases, and it can be concluded that all three elements have an effect on permeability estimation as shown in Figure 8 (b).

Table 3: Porosity, absolute permeability, formation factor, and cementation exponent values with respect to pore throat structure effects.

Case no.	Network Index	Description	Φ (fraction)	K_{ab} (md)	*FF*	*m* (assuming *a* = 1)
1	Ref. Network	Reference network (No clay & *Lp* = 2*Rp*)	0.153	2499	11.1	1.28
2	Case 1	Reducing pore radius	0.01	64.9	50.1	0.85
3	Case 2	Reducing throat radius	0.105	23.8	89	1.99
4	Case 3	Reducing coordination number	0.127	218	60.2	1.99
5	Case 4	Reducing pore & throat radius	0.006	11.8	131.6	0.95
6	Case 5	Reducing pore radius & coordination number	0.007	11.8	226.5	1.09
7	Case 6	Reducing throat radius & coordination number	0.101	1	626.9	2.81
8	Case 7	Reducing all factors combined	0.005	0.74	748	1.25

Overall, the value of formation factor increases with the reduction of these elements individually or combined as shown in Figure 8 (c). Combining the effect of reducing throat radius and decreasing number of flow pathways (coordination number) is causing a significant increase in the formation factor. Formation factor values are plotted against the estimated porosity for all the cases in semi-log and Cartesian scale as shown in Figure 9 (a) and Figure 9 (b) respectively.

Furthermore, at each porosity value, formation factor is estimated using Archie's equation assuming *m*=2.0 (for sandstone comprised of spherical grains) [36] and the values are plotted in the same figures. Because of the high level of variability in cementation exponent due to the difference in pore structure between these networks, data points do not follow the same power law and a linear function similar to those data points estimated with a constant value of *m*=2. However, the data points for those networks (Case 1, Case 4, Case 5, and Case 7) with similar and small pore size distribution have less scattering as shown in Figures 9 (a) and 9 (b). Case 2 and Case 3 have similar estimated value of cementation exponent (*m*=1.99) and this match could be anticipated with similarity in pore size distribution and the arrangement of pore space despite the difference in throat size and coordination number between these cases. Glover [37] interpreted the cementation exponent (*m*) as a function of the change rate of availability pathways for transport (Connectedness) with porosity and the arrangement of pore space (Connectivity). However, when the effect of reducing throat radius and coordination number is combined as shown in Case 5, a higher value of *m* is estimated; this is an equivalent representation to a carbonate pore structure. Furthermore, those networks (Case 1, Case 4, Case 5, and Case 7) having a similar reduced distribution of pore radius are plotted together as shown in Figures 9 (a) and (b), but they do not follow a similar power function. The reason is the difference in throat size and coordination number producing different values of *m*. Figure 9 (c) illustrates the relationship between formation factor and permeability. In general, the formation factor will decrease with increasing absolute permeability. Moreover, the networks are divided into two groups based on the coordination number distribution. Networks which were generated with a

reduced coordination number distribution (Case 3, Case 5, Case 6, and Case 7) are fitted well in a blue dash line, where the other networks (Base Case, Case 1, Case 2, and Case 4) consist of a higher distribution of coordination number and are plotted in a dark red dash line. Hence it can be concluded that the network connectivity (coordination number) factor affects the permeability-formation factor relationship more than the other factors. In Figure 9 (d), the cross-plot of absolute permeability versus porosity is plotted in log-log scale, and it can be seen that the data points are classified in two groups. Low porosity networks are plotted in the left side and the high porosity data points in the right side. This classification can be linked to the similarity of pore radius distribution used for generating these networks. Furthermore, pore topology/structure and pore throat radius are the major factors having influence on permeability estimation. Aguilera [38] developed an integrated cross-plot of permeability versus porosity according to pore throat aperture at 35% mercury saturation, which allows one to distinguish between flow units in conventional, tight gas, and shale gas reservoirs. Consequently, the data points are re-plotted as shown in Figure 10 (a) according to the throat size distribution used for generating the networks. The data points for the networks of Berea sandstone, Base Case, Case 1, Case 3, and Case 5 show correlation, but the data for the networks with lower permeability such as Case 2, Case 4, Case 6, and Case 7 are scattered around the fitted power function line. This could be due to the fact that the coordination number distributions are not the same for these networks. Figure 10 (b) illustrates the permeability-porosity relationship based on coordination number and throat radius distributions. Each of the two networks generated using similar throat radius and coordination number is plotted in the same curve.

Pore Throat Geometry Effects

The 3D pore network of Case 7 of the previous section is assumed as a reference network here and a representative pore network of tight porous media. Thus a study is conducted by nine constructed networks to assess the impact of varying pore and throat geometries on estimating porosity, absolute permeability, and formation factor. The reference network consists of mixed shapes of pores and throats. The proportion of pore shape is 1% square, 4% circular, and 95% triangular. Throat shape percentage is 8% square, 2% circular, and 90% triangular. This combination was adopted through trial and error, because it would lead to the best fit of the experimental results, as it will be shown below. Table 4 illustrates the difference in estimating porosity, absolute permeability, formation factor, and porosity exponent. A first observation that can be drawn from Table 4 is that throat shape has a more significant control on absolute permeability, whereas the type of pore shape influences network porosity estimation. The change in formation factor is controlled more by throat shape than the shape of pore.

Figure 11 (a, b, and c) shows the variation of net porosity, absolute permeability and formation factor values with respect to different shape selection for pores and throats. In Figure 11, triangular cross-section produces higher net porosity, absolute permeability, and cementation exponent but a lower formation factor, whereas square and circular cross-section similarly yield to lower values of net porosity, absolute permeability, and cementation exponent but a higher formation factor value. This finding could be related to the value of shape factor (G) that is determined based on the selected shape (circular, square, and triangular) of pores and throats.

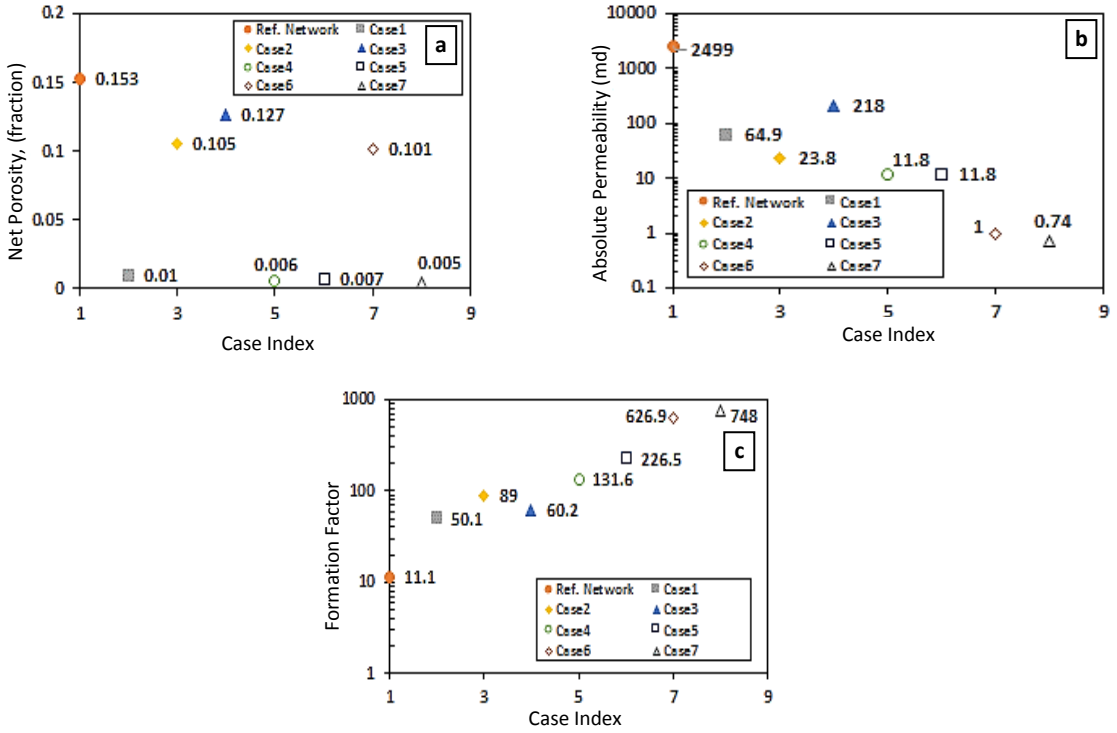

Figure 8: Pore structure (pore radius, throat radius, and coordination number) influence on (a) net porosity, (b) absolute permeability, and (c) formation factor estimation.

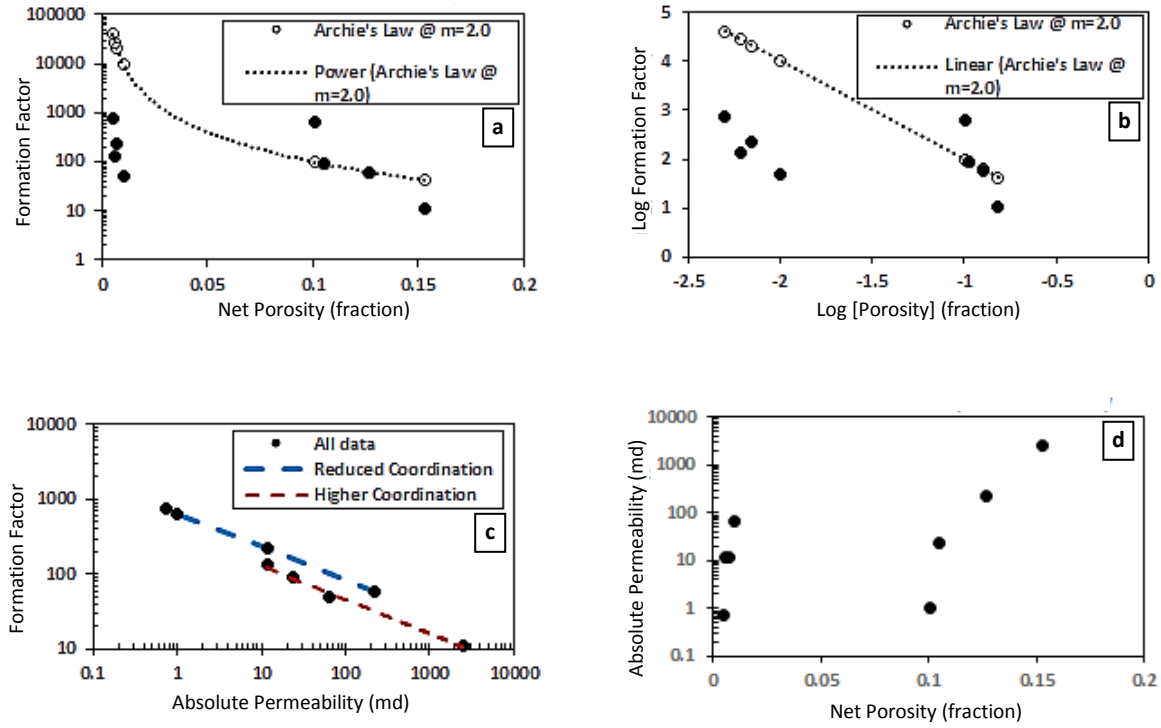

Figure 9: (a) Semi-log plot of the estimated values of formation factor vs. porosity for all the cases; the empty circle marker corresponds to Archie's Law estimation with *m*=2 and *a*=1; (b) Normal scale plot of Log(formation factor) vs. Log(porosity) for all the cases; (c) Log-Log plot showing the relationship between formation factor and permeability; (d) Semi-Log plot showing the relationship between estimated permeability and porosity for all the cases (individual cases are shown in Figure 10b).

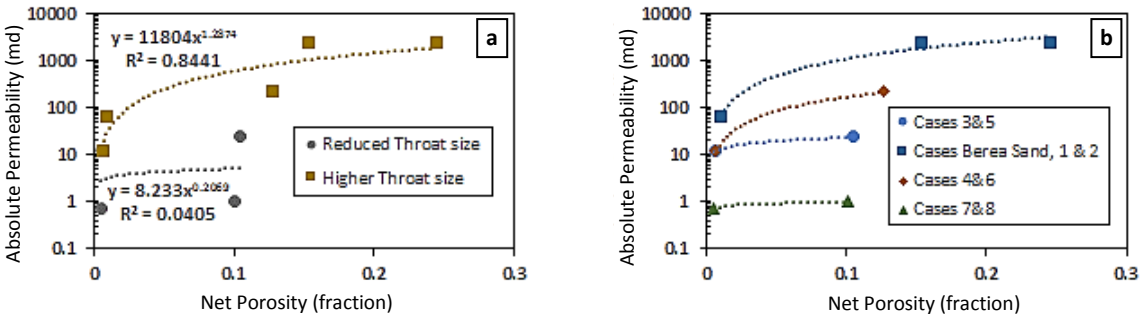

Figure 10: Cross-plot of absolute permeability vs. net porosity showing the relationship of the constructed networks based on throat size and coordination number distributions.

Table 4: Porosity, absolute permeability, formation factor, and cementation exponent values with respect to pore throat geometry effects.

Case Index	Throat Shape	Pore Shape	Φ (fraction)	K_{ab} (md)	*FF*	*m* (assuming *a* = 1)
1	Ref. Network	Ref. Network	0.005	0.74	748	1.249
2	100% Square	100% Triangular	0.003	0.36	1460.4	1.254
2		100% Square	0.002	0.36	1513.7	1.178
2		100% Circular	0.0019	0.35	1543	1.172
3	100% Circular	100% Triangular	0.003	0.25	1844	1.294
3		100% Square	0.0019	0.25	1897.8	1.205
3		100% Circular	0.0017	0.25	1927.4	1.186
4	100% Triangular	100% Triangular	0.0046	0.78	725.4	1.224
4		100% Square	0.0034	0.76	777.4	1.171
4		100% Circular	0.0031	0.75	805.6	1.158

The Imperial College software uses the dimensionless shape factor (*G*), as suggested by Mason and Morrow [39] to correct for wetting layer, conductivity, and calculate capillary entry pressure as a direct function of the pore shape using expressions derived by other works [14, 15, 18, 34, 39, 40]. The value of dimensionless shape factor assigned for circular and square is higher than for that of the triangular cross-section shape. For circular and square shape, the value of shape factor (*G*) is 1/4π and 1/16 respectively, but the value of *G* for triangular cross-section differs from 0 (slit-shaped) to 0.048 (equilateral triangle shape). From equation (2), the area of each element increases as the shape factor *(G)* decreases; thus the porosity, permeability, and cementation exponent values increase accordingly. The relationship between the estimated petrophysical properties was studied.

Figure 12 (a,b) demonstrates the relationship between formation factor and net porosity in log-log and Cartesian scale. In Cartesian plot, a polynomial function fits the data points better than the linear function. It is been found experimentally that in tight gas sands the relationship between formation factor and porosity differs from the power function [41]. Figure 12 (c) shows a decrease in the formation factor values as absolute permeability increases with respect to changing throat shape, while having a similar distribution of pore and throat radius and coordination number. There is no significant effect on permeability-formation factor relationship with changing pore geometries. In addition, the predicted absolute permeability values were plotted with net porosity as shown in Figure 12 (d). The pore geometries influence the permeability-porosity relationship in tight porous media considering that the

pore structure is the same for all the generated networks. Figure 13 (a) shows the data points for these networks plotted with the values of networks (Case 7 and Case 6) from the previous section having the same pore structure. However, better data fitting can be seen when plotting permeability and porosity values of a network (Case 3), which consists of 100% triangular cross-section shape of pores and throats with Case 6 and Case 7 as shown in Figure 13 (b). This good correlation is due to the fact that the majority of cross-section shape of pores and throats are triangular for both the generated reference network (Case 7) and network of Case 6.

Throat length significantly affects the estimation of electrical formation factor particularly in tight porous media. This effect is demonstrated by reconstructing the reference network and the network (Case 7) from the pore structure effect section by assuming that the connection path between connected pores is a straight line. Thus throat length is calculated based on the actual distance between the centers of two connected pores instead of varying the throat length obtained from Weibull equation. Table 5 demonstrates the variation of the estimated formation factor along with porosity and permeability through permeable and tight networks. It can be seen that as the length of throat is increasing, the value of porosity and permeability increase but formation factor value decreases. The effect is more significant for the case of tight network. Assuming a variable throat length in pore network modeling is more accurate than a straight-line path assumption, since the real pore space follows quite a tortuous path [42].

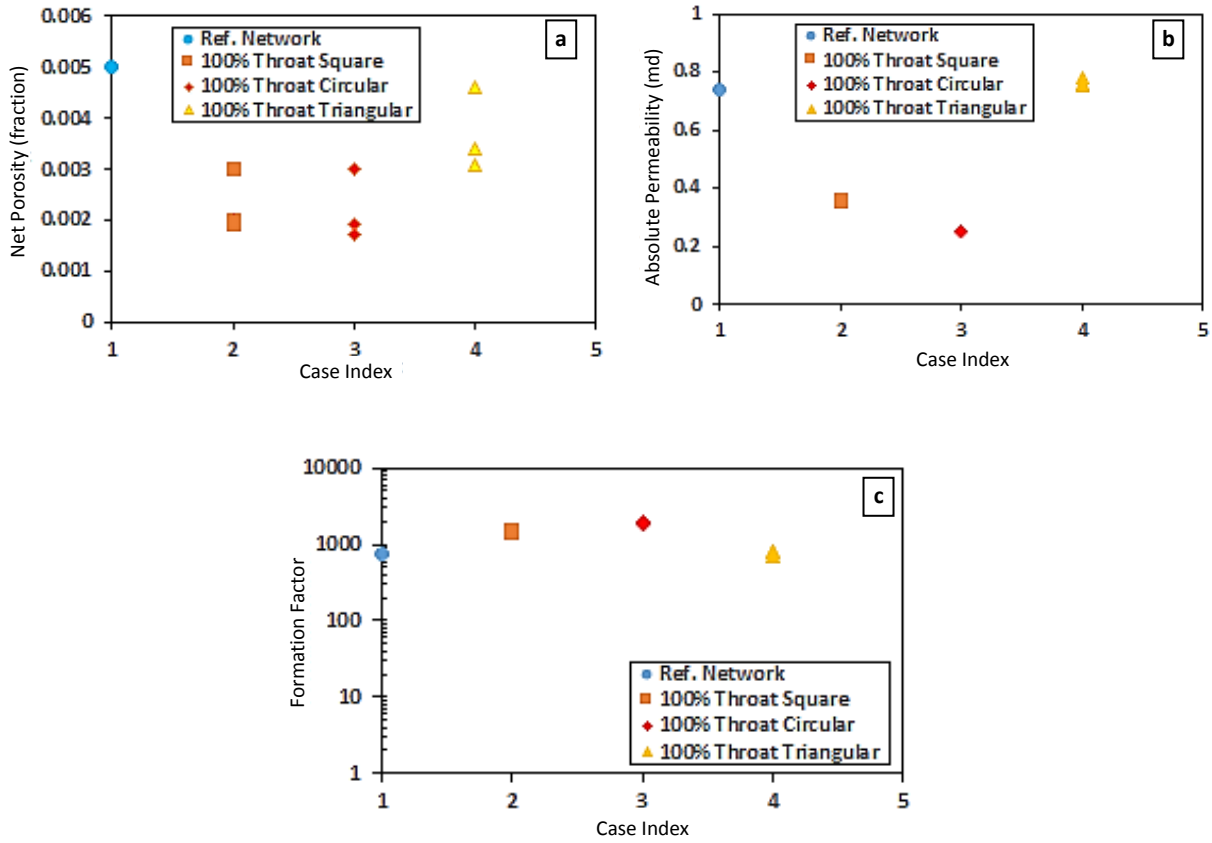

Figure 11: Influence of varying pore and throat geometries on (a) net porosity, (b) absolute permeability, and (c) formation factor estimation.

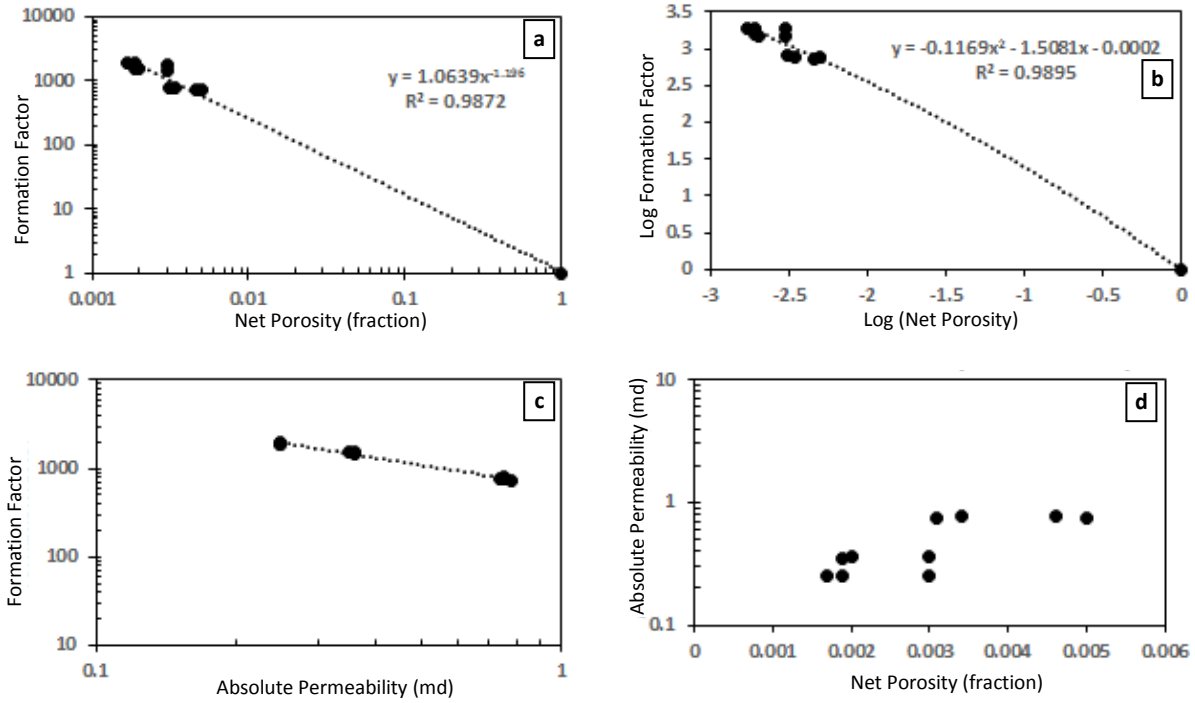

Figure 12: (a) Log-log plot for the estimated values of formation factor vs. porosity for all cases, (b) Normal scale plot for the estimated values of Log (formation factor) vs. Log (porosity), (c) Log-log plot showing the relationship between formation factor and absolute permeability, and (d) Semi-log plot showing the relationship between estimated absolute permeability and net porosity for all the cases.

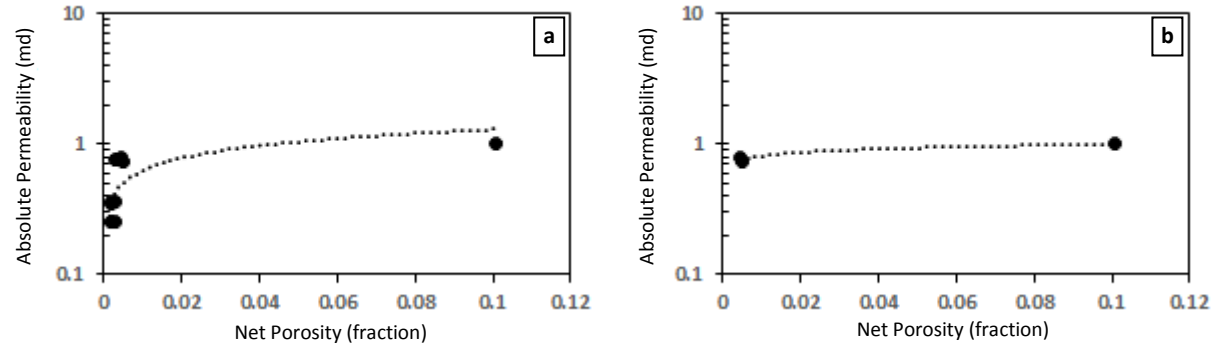

Figure 13: Cross-plot of absolute permeability vs. net porosity showing the influence of pore geometries on tight porous media considering pore structure equal for all the networks.

Tight Porous Media

According to the network in Case 7, eleven additional media are generated to assist in demonstrating the pore network capability to replicate the macroscopic properties relationships obtained experimentally by Byrnes et al. [26] in tight gas sandstones. In the generated networks, pore and throat geometries and coordination pore and throat radius vary based only on changing the Weibull coefficient (δ). Table 6 illustrates the estimated values of porosity, absolute permeability, and formation factor using Pore-Scale software and the cementation factor obtained by Archie's equation assuming a = 1.0.

Table 5: Porosity, permeability, and formation factor values for two different networks constructed using different assumptions in throat length estimation.

Throat Length Estimation Assumption	Network	Porosity (fraction)	K_{ab} (md)	FF	m (assuming a = 1)
Straight-line path	Ref. Network of pore structure test	0.237	998	26.5	2.28
Vary throat length		0.153	2499	11.1	1.28
Straight-line path	Network (Case 8), from pore structure test	0.01	0.19	2921	1.69
Vary throat length		0.005	0.74	748	1.25

Table 6: Porosity, absolute permeability, formation factor, and cementation exponent values as pore and throat radius distributions changed.

Tight Media No.	Porosity (fraction)	K_{ab} (md)	FF	m (assuming a = 1)
Media 1	0.071	2.83	376.3	2.24
Media 2	0.051	0.95	628.5	2.17
Media 3	0.034	0.344	1033.5	2.05
Media 4	0.021	0.149	1566.35	1.90
Media 5	0.012	0.071	2415.2	1.76
Media 6	0.0059	0.046	3082.15	1.57
Media 7	0.0058	0.0328	3785.8	1.60
Media 8	0.0026	0.035	3689.93	1.38
Media 9	0.0025	0.031	3994.4	1.38
Media 10	0.0016	0.0335	3712	1.28
Media 11	0.0011	0.033	3767.3	1.21

Figure 14 (a,b) shows the macroscopic properties the relationships of the generated tight networks with varying pore and throat size distributions. Clearly, the relationship of formation factor-porosity in tight porous media does not follow the power function line as shown in Figure 14 (a). Instead, the data points bend to the left in reference to Archie's Law line, and this behavior was also shown experimentally by Byrnes et al. and Liu et al. [26, 41]. Consequently, in Figure 14 (b), the porosity value decreases as cementation exponent drops. This relationship was characterized by a dual porosity model, in which the secondary pores represent the large fraction of the void space connected to each other by slots (fractures) [25, 36]. These two cross-plots are plotted with the experimental measurements of tight gas sandstone samples obtained by Byrnes et al. [26]. Obviously, the estimated points by pore network modeling follow the laboratory data points trend, but the pore network formation factor is higher as shown in Figure 15 (a,b). This inconsistently with formation factor estimation is either due to limited available pathways for flow or the long throat length used. Additionally, as the porosity of porous media got lower by altering network element properties, the porosity-formation factor correction is deviating from Archie's quadratic function as shown in Figure 15 (a). Figure 16 (a) emphasizes that the coordination number (connectivity) affects the formation factor–permeability relationship more than pore and throat sizes. Considering this cross-plot, there is an inverse relationship and the data points fall on the same line. Figure 16 (b) shows the cross-plot of

permeability vs. porosity in semi-log scale. The data points are fit in a single line using exponent correlation. However, data points having low absolute permeability estimation do not fall well on the same fitted correlation. This behavior is observed as shown in Figure 12 (d) and Figure 13 (a).

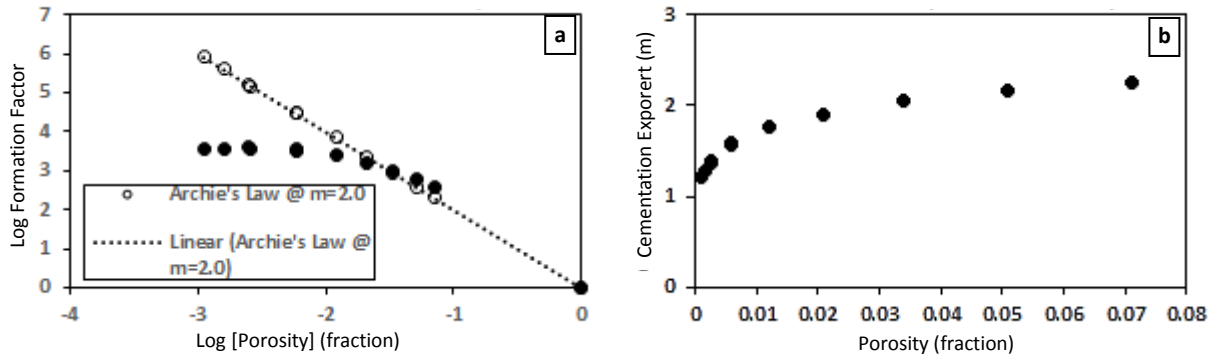

Figure 14: (a) Normal scale plot of the estimated values of Log (formation factor) vs. Log (porosity) and (b) Cementation exponent–porosity cross-plot.

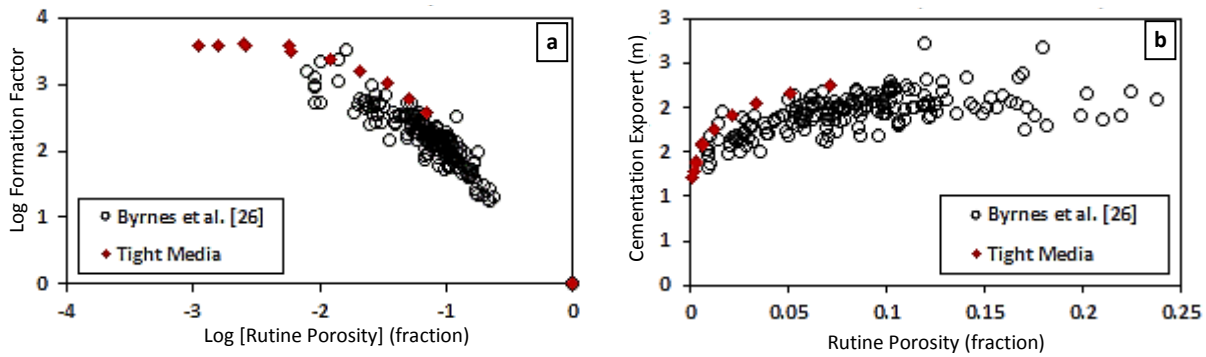

Figure 15: Pore network estimation is consistent with laboratory measurements; (a) Formation factor-porosity cross-plot and (b) Cementation exponent (*m*)-porosity cross-plot.

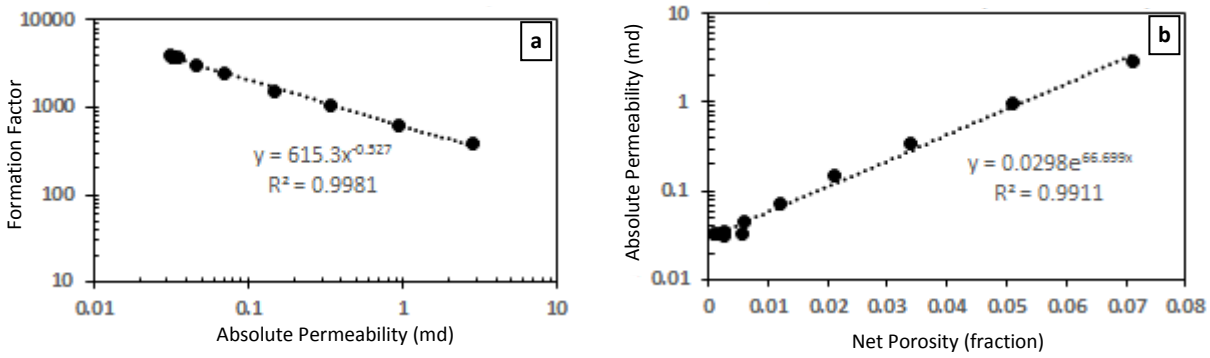

Figure 16: (a) Log-log plot showing formation factor and absolute permeability relationship and (b) Semi-log plot showing the relationship between estimated absolute permeability and net porosity for all the networks.

CONCLUSIONS

It can be concluded that pore network modeling approach has the ability to construct equivalent 3D pore networks of a real porous media and mimic the physics of fluid flow at pore scale level. Eventually, it offers the flexibility to study macroscopic properties relationships with pore throat structure and geometries through simple and complex pore structure of real rock. Thus, in the current work, it has been shown that:

- A good match with laboratory measurements of Berea sandstone was achieved. The match of capillary pressure and resistivity index could not be made, since the laboratory data for this were not available.
- Assuming that the pore length is twice the pore radius results in a reduction of porosity, absolute permeability, and formation factor.
- Reducing pore size distribution substantially decreases the net porosity value and the combined reduction of throat size and coordination number significantly increases formation factor value but decreases the value of absolute permeability.
- Connectivity should be considered beside throat size for a better classification in permeability-porosity cross-plot.
- Triangular cross-section will produce higher values of network porosity, absolute permeability, and cementation exponent but a lower formation factor compared to square and circular cross-sections, which yield lower values of net porosity, absolute permeability, and cementation exponent but a higher formation factor.
- The shape geometry of throats controls significantly absolute permeability and formation factor, whereas the shape of pores influences the porosity estimation and have a less impact on formation factor.
- Formation factor-absolute permeability relationship with varying pore and throat geometries follows the similar relationship obtained with changing pore structure. This is due to the assumption that formation factor will vary inversely with absolute permeability made by pore-scale modeling simulator.
- Formation factor-porosity cross-plot differs from power function in tight porous media. The data will bend to the left with decreasing porosity.
- Finally, a variable throat length is the proper way to reflect pore scale tortuosity, especially for tight porous media.

ACKNOWLEDGEMENTS

The authors acknowledge Saudi Aramco for the financial support and Professor Martin Blunt for the valuable discussions.

NOMENCLATURE

a	Archie constant (dimensionless)
A	Area (m^2)
$Clayvol$	Clay volume (m^3)
$Clayper$	Clay proportion (fraction)
F	Formation factor (dimensionless)
G	Dimensionless shape factor
K_{ab}	Absolute permeability (md)
K_{rw}	Relative permeability of water
K_{ro}	Relative permeability of oil
P_c	Capillary pressure (Pa)
I	Resistivity index
L	Length of pore or throat (m)
m	Cementation exponent
r	radius (m)
x	Estimated property value by Weibull Equation
x_{max}	Maximum value of x property
x_{min}	Minimum value of x property
Φ	Porosity (fraction)

Subscripts

ab	Absolute

p	Pore

Greek Symbols

δ	Weibull exponent constant
γ	Weibull exponent constant

REFERENCES

[1] Okabe H. and Blunt M. J., "Pore Space Reconstruction Using Multiple-point Statistics," *Journal of Petroleum Science and Engineering*, **2005**, *46*, 121-137.

[2] Okabe H., "Pore-scale modeling of carbonates," Ph.D. Thesis, Imperial College, London, United Kingdom, **2004**.

[3] Blunt M. J., "Flow in Porous Media Pore-network Models and Multiphase Flow," *Current Opinion in Colloid & Interface Science*, **2001**, *6*, 197-207.

[4] Blunt M. J., Jackson M. D., Piri M., and Valvatne P. H., "Detailed Physics, Predictive Capabilities and Macroscopic Consequences for Pore-network Models of Multiphase Flow," *Advances in Water Resources*, **2002**, *25*, 1069-1089.

[5] Celia M. A., Reeves P. C., and Ferrand L. A., "Recent Advances in Pore Scale Models for Multiphase Flow in Porous Media," *Review of Geophysics*, **1995**, *33*, 1049-1057.

[6] Fatt I., "The Network Model of Porous Media," *Petroleum Transactions of AIME,* **1956**, *207*, 144-181.

[7] Chatzis I. and Dullien F. A. L., "Modeling Pore Structure by 2-D and 3-D Networks with Application to Sandstones," *Journal of Canadian Petroleum Technology*, **1977**, *16*, 97-108.

[8] Dixit A. B., McDougall S. R., and Sorbie K. S., "A Pore-level Investigation of Relative Permeability Hysteresis in Water-wet Systems," *SPE Journal*, **1998**, *3*, 115- 123.

[9] Grattoni C. A. and Dawe R. A., "Pore Structure Influence on the Electrical Resistivity of Saturated Porous Media," in the *SPE Latin America/Caribbean Petroleum Engineering Conference* SPE 27044*,* **1994**.

[10] Jerauld G. R. and Salter S. J., "The Effect of Pore-structure on Hysteresis in Relative Permeability and Capillary Pressure: Pore-level Modeling," *Transport in Porous Media*, **1990**, *5*, 103-151.

[11] Lowry M. I. and Miller C. T., "Pore-scale Modeling of Non-wetting-phase Residual in Porous Media," *Water Resources Research*, **1995**, *31*, 455-473.

[12] Ören P. E. and Bakke S., "Process Based Reconstruction of Sandstones and Prediction of Transport Properties," *Transport in Porous Media*, **2002**, *46*, 311-343.

[13] Ören P. E. and Bakke S., "Reconstruction of Berea Sandstone and Pore-Scale Modeling of Wettability Effects," *Journal of Petroleum Science and Engineering*, **2003**, *39*, 177-199.

[14] Ören P. E., Bakke S., and Arntzen O. J., "Extending Predictive Capabilities to Network Models," *SPE Journal*, **1998**, *3*, 324-336.

[15] Patzek T. W., "Verification of a Complete Pore Network Simulator of Drainage and Imbibitions," *SPE Journal*, **2001**, *6*, 144-156.

[16] Piri M. and Blunt M. J., "Three-Dimensional Mixed-wet Random Pore-scale Network Modeling of Two-and Three-phase Flow in Porous Media: Model Description," *Physical Review*, **2005,** *71*.

[17] Piri M. and Blunt M. J., "Three-Dimensional Mixed-wet Random Pore-Scale Network Modeling of Two-and Three-phase Flow in Porous Media. II. Results," *Physical Review*, **2005**, *71*.

[18] Valvatne P. H. and Blunt M. J., "Predictive Pore-scale Network Modeling," in the *SPE Annual Technical Conference and Exhibition*, held in Denver CO., SPE 84550, **2003**, 5-8.

[19] Bakke S. and Ören P. E., "3-D Pore-scale Modeling of Sandstones and Flow Simulations in the Pore Networks," *SPE Journal*, **1997**, *2*, 136-149.

[20] Al-Kharusi A. S. and Blunt M. J., "Network Extraction from Sandstone and Carbonate Pore Space Images," *Journal of Petroleum Science and Engineering*, **2007**, *56*, 219-231.

[21] Dong H. and Blunt M. J., "Pore-network Extraction from Micro-computerized-tomography Images," *Physical Review E*, **2009**, *80*, 197-216.

[22] Chen S. and Gary D. D., "Lattice Boltzmann method for fluid flows," *Annual Review of Fluid Mechanics,* **1998**, *30*, 329-364.

[23] Gunstensen A. K. and Daniel H. R., "Lattice-Boltzmann Studies of Immiscible Two-phase Flow through Porous Media," *Journal of Geophysical Research: Solid Earth,* **1993**, *98*, 6431-6441.

[24] Hazlett R. D., Chen S. Y., and Soll W. E., "Wettability and Rate Effects on Immiscible Displacement: Lattice Boltzmann Simulation in Microtomographic Images of Reservoir Rocks," *Journal of Petroleum Science and Engineering,* 1998, *20*, 167-175.

[25] Aguilera R., "Role of Natural Fractures and Slot Porosity on Tight Gas Sands," in the *SPE Unconventional Reservoirs Conference*, Society of Petroleum Engineers SPE 114174, **2008**.

[26] Byrnes P. A., Cluff R. M., and Webb J. C., "Analysis of Critical Permeability, Capillary and Electrical Properties for Mesaverde Tight Gas Sandstones from Western US Basins," Final Scientific/ Technical Report submitted to DOE and NETL, **2009**.

[27] Soeder D. and Randolph P., "Porosity, Permeability and Pore Structure of the Tight Mesaverde Sandstone, Piceance Basin and Colorado," *SPE Formation Evaluation*, **1987**, *2*, 129-136.

[28] Idowu N. A., "Pore-Scale Modeling: Stochastic Network Generation and Modeling of Rate Effects in Water Flooding," Ph.D. Thesis, Imperial College London, United Kingdom, **2009**.

[29] Mehmani A., Prodanović M., and Javadpour F., "Multiscale, Multiphysics Network Modeling of Shale Matrix Gas Flows," *Transport in Porous Media*, **2013**, *99*, 377-390.

[30] Mehmani A., Tokan-Lawal A., Prodanovic M., and Sheppard A., "The Effect of Microporosity on Transport Properties in Tight Reservoirs," *in SPE North American Unconventional Gas Conference and Exhibition*, SPE 144384, **2011**.

[31] Rahmanian M., "Pore Level Study of Tight Formations," M.SC. Thesis, University of Calgary, Canada, **2011**.

[32] Kantzas A. and Chatzis I., "Application of the Conjugate Gradients Method in the Simulation of Relative Permeability Properties of Porous Media," *Chemical Engineering Communication*, **1988**, *69*, 169-189.

[33] Kantzas A. and Chatzis I., "Network Simulation of Relative Permeability Curves Using a Bond Correlated-site Percolation Method of Pore Structure," *Chemical Engineering Communication*, **1988**, *69*, 191-214.

[34] Valvatne P. H., "Predictive Pore-scale Modelling of Multiphase Flow," Ph.D. Thesis, Imperial College London, United Kingdom, **2004**.

[35] Al-Dhahli A. R., Geiger S., and van Dijke M. I., "Three-phase Pore-network Modeling for Reservoirs with Arbitrary Wettability," *SPE Journal*, **2012**, *18*, 285-295.

[36] Cluff R. M., Byrnes A. P., Whittaker S., and Krygowski D., "Evidence for a Variable Archie Porosity Exponent '*m*' and Impact on Saturation Calculations for Mesaverde Tight Gas Sandstones: Piceance, Uinta,

Green River, Wind River, and Powder River Basins," In *Proceedings of the AAPG Rocky Mountain Section Meeting*, Denver, Colorado, **2008.**

[37] Glover P., "What is the Cementation Exponent? A New Interpretation," *The Leading Edge*, **2009**, *28*, 82-85.

[38] Aguilera R., "Flow Units: from Conventional to Tight Gas to Shale Gas Reservoirs," in the *Trinidad and Tobago Energy Resources Conference*, Society of Petroleum Engineers SPE 132845, **2010**.

[39] Mason G. and Morrow N. R., "Capillary Behavior of a Perfectly Wetting Liquid in Irregular Triangular Tubes," *Journal of Colloid and Interface Science*, **1991**, *141*, 262-274.

[40] Ma S., Mason G., and Morrow N. R., "Effect of Contact Angle on Drainage and Imbibition in Regular Polygonal Tubes," *Colloids and Surfaces A: Physicochemical and Engineering Aspects*, **1996**, *117*, 273-291.

[41] Liu X.P., Hu X.X., and Xiao L., "Effects of Pore Structure to Electrical Properties in Tight Gas Reservoirs: An Experimental Study," presented in the *SPE/EAGE European Unconventional Resources Conference and Exhibition held in Vienna* SPE 150926, **2012**.

[42] Blunt M. J., Personal Communication, **2014.**